Blood Cells, Molecules and Diseases 77 (2019) 61–66

Contents lists available at ScienceDirect

Blood Cells, Molecules and Diseases

journal homepage: www.elsevier.com/locate/bcmd

Evidence for three populations of the glucose transporter in the human erythrocyte membrane

Gayani C. Kodippili[a], Karson S. Putt[b], Philip S. Low[a,b,*]

[a] Department of Chemistry, Purdue University, West Lafayette, IN 47907, USA
[b] Institute for Drug Discovery, Purdue University, West Lafayette, IN 47907, USA

ARTICLE INFO

Editor: Mohandas Narla

Keywords:
Glucose transporter 1
GLUT1
Band 3
Single particle tracking
Erythrocyte membrane structure

ABSTRACT

Glucose transporter 1 (GLUT1) is one of 13 members of the human equilibrative glucose transport protein family and the only glucose transporter thought to be expressed in human erythrocyte membranes. Although GLUT1 has been shown to be anchored to adducin at the junctional spectrin-actin complex of the membrane through interactions with multiple proteins, whether other populations of GLUT1 also exist in the human erythrocyte membrane has not been examined. Because GLUT1 plays such a critical role in erythrocyte biology and since it comprises 10% of the total membrane protein, we undertook to evaluate the subpopulations of erythrocyte GLUT1 using single particle tracking. By monitoring the diffusion of individual AlexaFluor 488-labeled GLUT1 molecules on the surfaces of intact erythrocytes, we are able to identify three distinct subpopulations of GLUT1. While the mobility of the major subpopulation is similar to that of the anion transporter, band 3, both a more mobile and more anchored subpopulation also exist. From these studies, we conclude that ~65% of GLUT1 resides in similar or perhaps the same protein complex as band 3, while the remaining 1/3rd are either freely diffusing or interacting with other cytoskeletally anchored membrane protein complexes.

1. Introduction

Erythrocyte membrane proteins or their orthologs are found in almost all cells of the body [1,2]. Because of this compositional similarity and the erythrocyte membrane's accessibility, the red blood cell membrane (RBCM) has served as a crude model for mammalian plasma membranes for many years [2,3,4,5].

Current models of the red blood cell membrane (RBCM) depict a lipid bilayer embedded with a diversity of membrane-spanning proteins anchored to a cortical spectrin cytoskeleton via several bridging molecules such as ankyrin, adducin, protein 4.1 and protein 4.2 [3,4]. Most diagrams of the membrane also show a glucose transporter (GLUT1) anchored to adducin at the junctional spectrin-actin complex [3,4]. Indeed, an interaction between GLUT1, adducin and dematin seems assured based on surface labeling, immunoprecipitation, and proteomic studies [5]. However, GLUT1 also has been proposed to interact with other RBCM proteins, including the cytoplasmic domain of band 3 [6] and stomatin [7], suggesting its association with the membrane may not be so simplistic.

Based on past studies demonstrating that different motile populations of membrane-spanning proteins can be characterized by “single particle tracking” experiments, where the diffusion paths of the different populations are imaged and their diffusions coefficients calculated from diffusion trajectories as a function of time [8], we undertook to determine the motile population(s) of GLUT1 in the RBCM. In the studies below, we covalently react a GLUT1-specific biotinylated ligand, ATB-BMPA [9] with glucose transporters in intact RBCs and then employ a streptavidin-linked fluorophore to track the movement of single GLUT1 molecules in intact RBCs. The data we obtain demonstrate that there are at least 3 subpopulations of GLUT1 in the membranes of whole RBCs and that only one subpopulation diffuses with a diffusion coefficient similar to that of adducin-associated band 3.

2. Materials and methods

2.1. Materials

The photoactivatable biotin-conjugated ATB-BMPA (N-[2-[2-[2-[(N-Biotinyl-caproylamino)-ethoxy)ethoxyl]-4-[2-(trifluoromethyl)-3H-diazirin-3-yl]benzoyl]-1,3-bis(mannopyranosyl-4-yloxy)-2-propylamine) was purchased from Toronto Research Chemicals Inc. (North York, Ontario, Canada). Streptavidin-conjugated Q-dot 525 was purchased from Invitrogen (Waltham, MA). All other materials were purchased from Thermo-Fisher (Waltham, MA).

* Corresponding author at: Department of Chemistry, Purdue University, 560 Oval Drive, West Lafayette, IN 47907, USA.
E-mail address: plow@purdue.edu (P.S. Low).

https://doi.org/10.1016/j.bcmd.2019.03.005
Received 25 February 2019; Received in revised form 22 March 2019; Accepted 23 March 2019
Available online 29 March 2019
1079-9796/

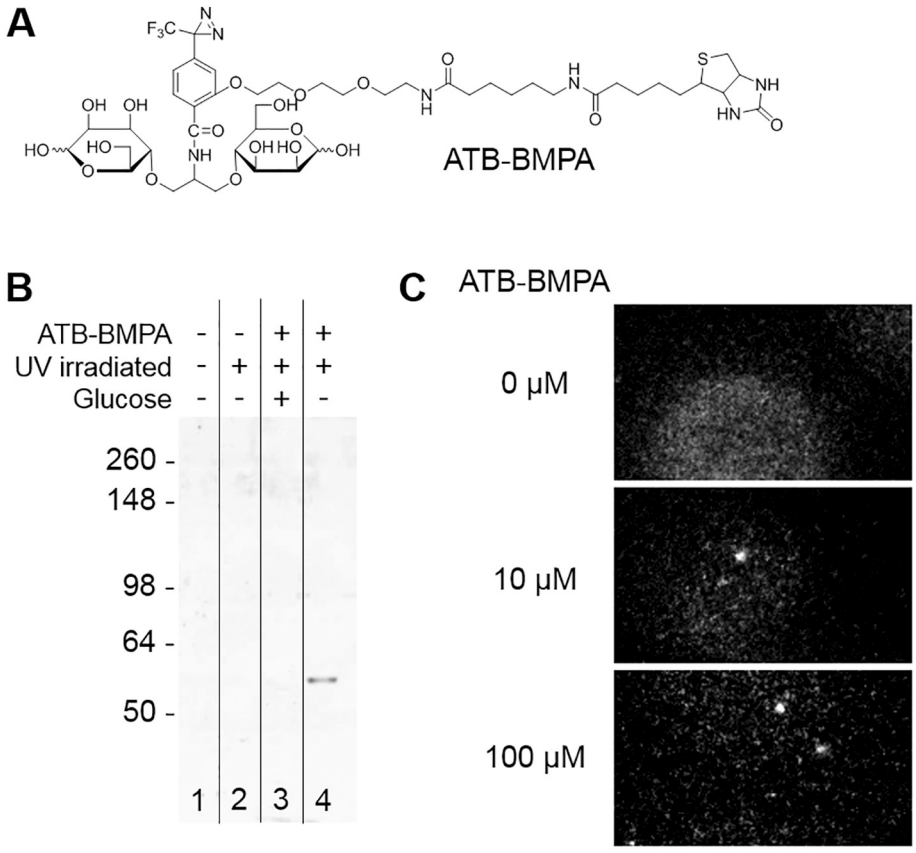

Fig. 1. Single particle labeling of human RBCs. A) Chemical structure of ATB-BMPA, a selective GLUT1 binder linked to a photo-crosslinking moiety and biotin. B) Erythrocytes were treated with ATB-BMPA then UV irradiated to crosslink the molecule to any proteins to which it was bound in the presence or absence of competing glucose. Cells were lysed and a western blot was performed utilizing streptavidin-conjugated with Horse Radish Peroxidase to detect the presence of covalently attached ATB-BMPA. C) Erythrocytes were treated with various concentrations of ATB-BMPA, UV irradiated to crosslink the ATB-BMPA with any proteins to which it was bound, washed, and imaged via confocal microscopy.

2.2. Labeling of GLUT1 and band 3 in intact human erythrocytes with fluorescent tracers

Blood samples from healthy volunteers were drawn following informed consent and approval by Purdue University's Institutional Review Board. Blood was centrifuged at 1000*g* to pellet the erythrocytes. The plasma and white cell fractions (buffy coat) were discarded. Erythrocytes were washed 3× with phosphate buffered saline, pH 7.4, lacking glucose and then diluted to 5% hematocrit in the same buffer. For labeling of GLUT1, washed RBCs were incubated with the desired concentrations of biotinylated ATB-BMPA at room temperature for 12 min in the dark. Cells then were irradiated with a 300 nm light source for 30 s, then 2 min and finally 4 min to promote covalent reaction of the compound with GLUT1. Unbound biotinylated ATB-BMPA was removed by washing erythrocytes 2× with PBS containing 0.1% BSA. Labeled cells then were incubated with streptavidin-conjugated Alexa-Fluor 488 at room temperature for 30 min followed by washing 2× with PBS. For single particle tracking, labeled cells were allowed to settle onto pre-cleaned, poly-lysine-coated cover slips positioned in a custom-built imaging chamber, and unattached cells were washed away with PBS containing 0.1% BSA. Finally, 500 μL of PBS was added to the chamber and the cells were imaged as described below. For labeling of the anion transport protein, band 3, washed RBCs were reacted with a DIDS-biotin (4,4′-diisothiocyano-2,2′-stilbenedisulfonic acid) conjugate and then derivatized with streptavidin-conjugated Q-dot 525 exactly as described previously [10].

2.3. SDS-PAGE and western blotting

Erythrocytes were prepared at 5% hematocrit in SDS-PAGE sample buffer containing 5% β-mercapto ethanol and separated electrophoretically on 10% SDS-PAGE gels. Proteins were transferred to a nitrocellulose membrane, blocked overnight in Tris-buffered saline containing 0.05% Tween 20 and 5% powdered milk, and washed 3× in Tris-buffered saline prior to staining with streptavidin-conjugated to horseradish peroxidase.

2.4. Single particle tracking via fluorescence video microscopy

Single particle tracking experiments were performed on an Olympus IX-71 inverted microscope (Olympus, Center Valley, PA) maintained at 37 °C in a temperature-controlled environment largely as described previously [10,11,12,13]. Oblique angle fluorescence imaging was used to excite single fluorophores or quantum dots for GLUT1 or band 3 tracking, respectively, on the apical surfaces of immobilized erythrocytes. The 488 nm Argon excitation laser (Newport, Irvine, CA) was expanded, filtered with a 488/10 nm line width bandpass filter (Chroma, Bellows Falls, VT), and directed towards the 100× microscope objective (PlanApo, NA 1.45 TIRFM oil immersion) parallel but off the optical axis through a 500 nm cutoff dichroic mirror (Chroma, Bellows Falls, VT). The resultant fluorescence image was projected through the dichroic mirror and a 525/50 nm bandpass emission filter (Chroma, Bellows Falls, VT), and the image was collected with a dual MCP intensified, cooled CCD camera (XR/Turbo-120z, Stanford Photonics, Inc., Palo Alto, CA). The excitation beam was positioned just outside of the condition for total internal reflection, thus allowing for a deeper excitation while still reducing background fluorescence arising from fluorescent matter in solution. Data were collected from the fluorophores attached to the top of the cell at 30, 120, 260, 400 and 1000 frames per second. Each movie was recorded for 1000 frames. Only particles whose trajectories were at least 40 frames long were chosen for analysis, which only provide a brief snapshot of protein behavior in the membrane. The trajectories were collected on a random selection of erythrocytes in each sample. In general, 100 to 500 RBCs were analyzed in each sample.

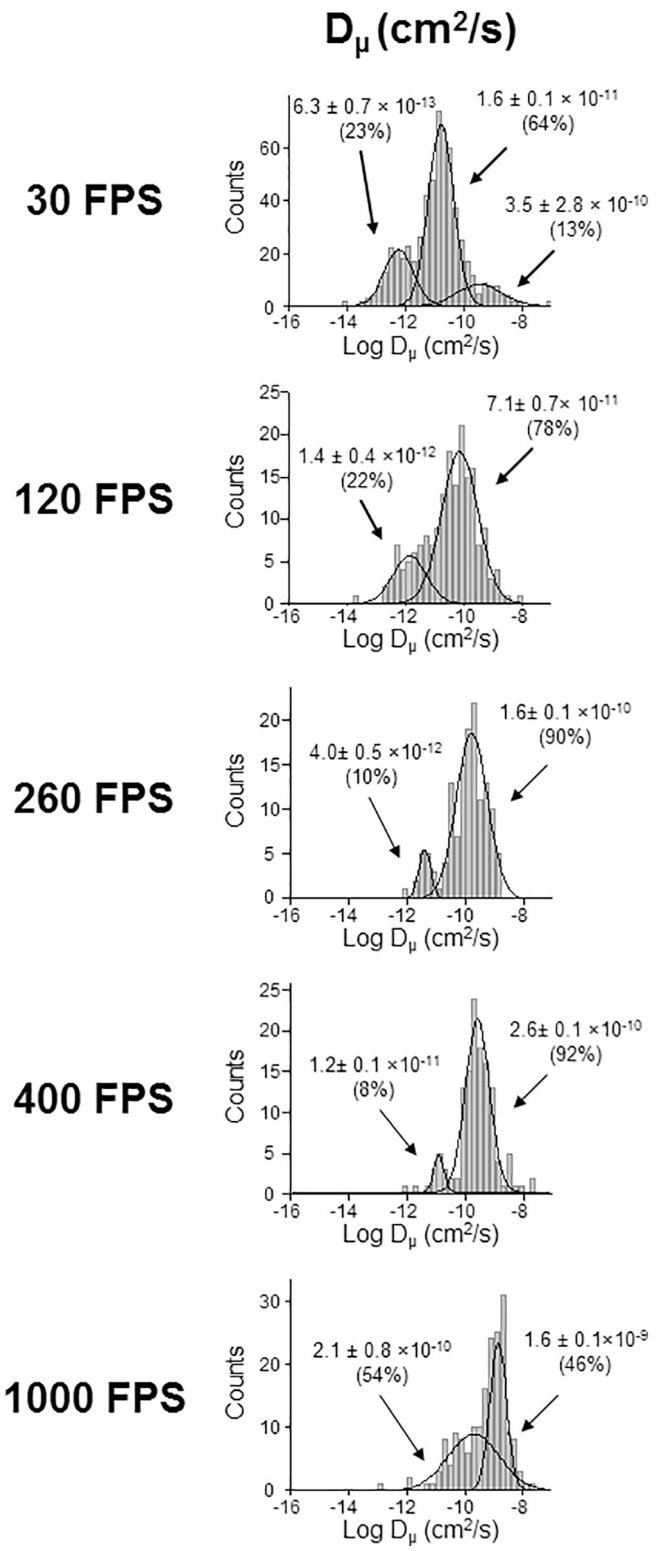

Fig. 2. Comparison of microscopic diffusion rates of GLUT1 from single particle tracking measurements at various frame rates. ATB-BMPA was covalently attached to GLUT-1 on the external surface of immobilized erythrocytes. Cells with a single fluorophore were imaged at various frame rates and the diffusion characteristics were determined.

2.5. Analysis of mobility

The position of the fluorophore in each video frame was determined using a Gaussian distribution of thresholded intensities as described previously [14]. Assessment of the mobility of the fluorophore was calculated from the mean-square displacement (MSD) of each trajectory between consecutive frames [15,16,17,18]. To determine the microscopic diffusion coefficient (D_μ), the asymptotic macroscopic coefficient (D_M), and the average spacing between barriers (compartment size), plots of the MSD vs time were fit with an approximation of the diffusion through an infinite array of partially permeable barriers [17]. Gaussian fits of the D_μ, D_M, and compartment size populations were utilized to determine the mean values.

3. Results and discussion

3.1. Selective single particle labeling of GLUT1 in human erythrocyte membranes by ATB-BMPA

In order to analyze the different motile populations of GLUT1, a fluorescent probe was required that reacts covalently and exclusively with GLUT1. Fortunately, a commercially available mannose probe linked to biotin and a photoaffinity moiety, ATB-BMPA [9], was commercially available and has been used to specifically label GLUT1 in several previous studies [19,20,21]. The structure of ATB-BMPA can be found in Fig. 1A. To confirm the selectivity and covalent binding of ATB-BMPA, erythrocytes were incubated with ATB-BMPA and irradiated in the presence or absence of competing glucose. Cells then were lysed and western blotting was performed using streptavidin as the probe. As shown in Fig. 1B, a single band at the expected molecular weight of GLUT1 (~55 kDa) was observed. Importantly, this band was not seen in preparations from cells incubated with competing glucose, indicating that ATB-BMPA is indeed selectively and covalently binding to GLUT1.

Next, erythrocytes were incubated with multiple concentrations of ATB-BMPA to determine a concentration where the majority of RBCs were only labeled with a single ATB-BMPA. As shown in the representative images in Fig. 1C, erythrocytes labeled with 10 μM ATB-BMPA exhibited mostly a single fluorescent tag per cell, whereas cell suspensions treated with 100 μM ATB-BMPA displayed a significant fraction of the cells with multiple fluorophores per cell. Therefore, a concentration of 10 μM ATB-BMPA was used for all further experiments. With a GLUT1 selective probe identified and a concentration that would predominately label only a single GLUT1 per erythrocyte, single particle tracking measurements could now be obtained and accurate diffusion characteristics determined.

3.2. Analysis of GLUT1 mobility at different frame rates

As shown in Fig. 2, the distribution of measured diffusion coefficients for labeled GLUT1 changes in relation to the frame rate used to acquire videos. The reason for this variability can be best understood by picturing two populations of GLUT1: 1) where one population is tethered to the spectrin-actin cytoskeleton and oscillating in place, and 2) a second population that is freely diffusing and slowly migrating across the cell surface. At a frame rate of 1000 frames per second (FPS), both GLUT1 molecules might move perhaps 10 nm between the first and second video frames (i.e. during the first 0.001 s). The GLUT1 that is anchored to the cytoskeleton will likely oscillate back to its original position between the second and third frames, while the GLUT1 that is freely diffusing may move an additional 10 nm further away during this same time interval. However, they will both be seen to move 10 nm per frame. A continuation of these motions will eventually lead to measurement of a similar diffusion coefficient for both populations of GLUT1, even though one is “wiggling” in place while the other is diffusing across the cell. In contrast, if the same two GLUT1 molecules are monitored at a frame rate of 30 FPS, the anchored population will be seen to have only diffused ~10 nm during the 0.033 s, while the freely diffusing GLUT1 could have migrated up to 330 nm during the same time interval; i.e. forcing the conclusion that the two populations of

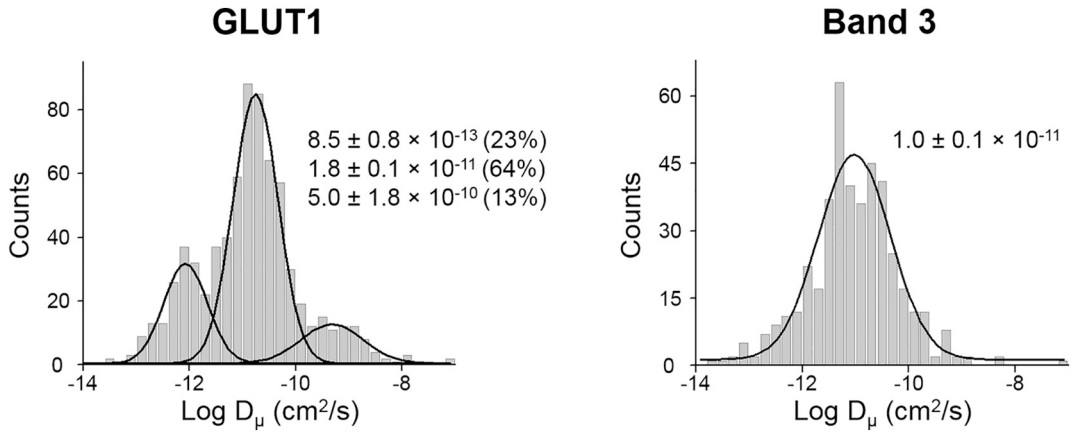

Fig. 3. Comparison of microscopic diffusion rates of GLUT1 and band 3 from single particle tracking measurements at 30 FPS. ATB-BMPA was covalently attached to GLUT-1 on the external surface of immobilized erythrocytes and incubated with streptavidin-conjugated Alexa Fluor 488. DIDS-biotin and streptavidin-conjugated Q-dot 525 were utilized to image band 3. Cells with a single fluorophore were imaged at 30 FPS and the diffusion characteristics were determined.

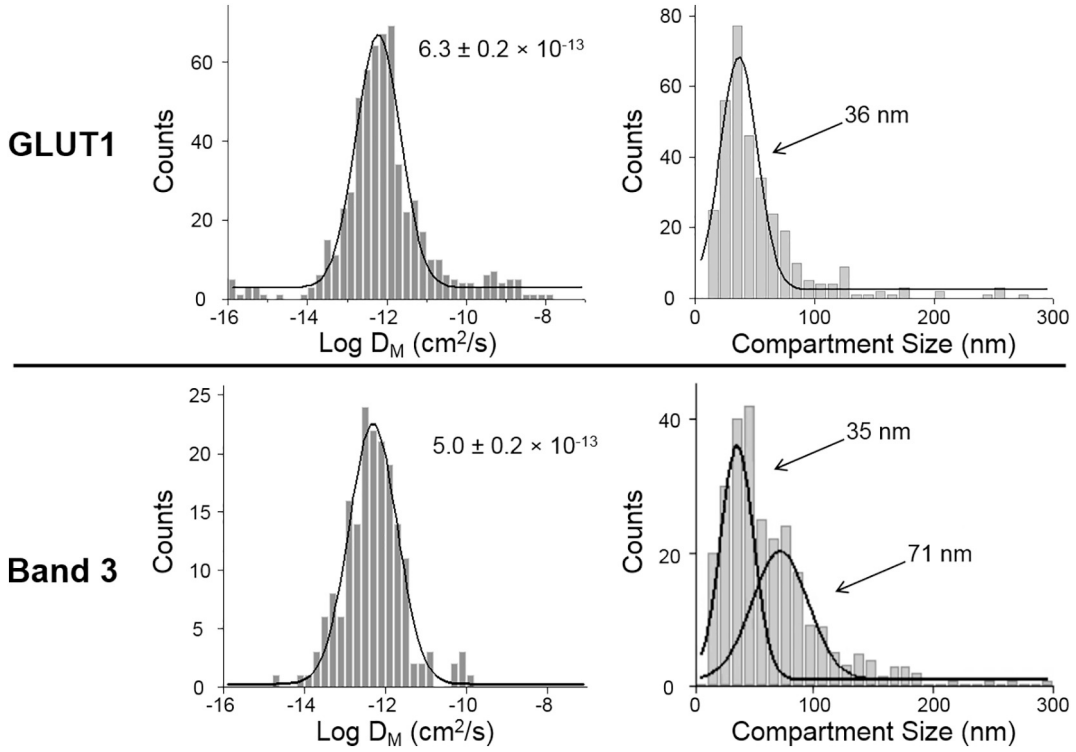

Fig. 4. Macroscopic diffusion rates and compartment sizes of GLUT1 and band 3 from single particle tracking measurements at 30 FPS. ATB-BMPA was covalently attached to GLUT1 on the external surface of immobilized erythrocytes and incubated with streptavidin-conjugated Alexa Fluor 488. DIDS-biotin and streptavidin-conjugated Q-dot 525 was utilized to image band 3. Cells with a single fluorophore were imaged at 30 FPS and the diffusion characteristics were determined.

Table 1
Microscopic diffusion rates, macroscopic diffusion rates, and compartment sizes of GLUT1 and band 3 from single particle tracking measurements.

Camera Speed	Protein	D_μ (cm^2/s)		D_M (cm^2/s)		Compartment size (nm)
		Fraction (%)	D_μ	Fraction (%)	D_M	
30 FPS	GLUT1	23%	8.5 +/- 0.8 x 10^{-13}	100%	6.3 +/- 0.2 x 10^{-13}	36 nm
		64%	1.8 +/- 0.1 x 10^{-11}			
		13%	5.0 +/- 1.8 x 10^{-10}			
	Band 3	100%	1.0 +/- 0.1 x 10^{-11}	100%	5.0 +/- 0.2 x 10^{-13}	35 nm 71 nm
120 FPS	GLUT1	22%	1.4 +/- 0.4 x 10^{-12}	100%	2.0 +/- 0.1 x 10^{-12}	39 nm
		78%	7.1 +/- 0.7 x 10^{-11}			
	Band 3	61%	1.6 +/- 1.6 x 10^{-11}	100%	1.7 +/- 0.1 x 10^{-12}	35 nm
		39%	2.1 +/- 0.4 x 10^{-10}			71 nm

GLUT1 are diffusing at very different rates. Thus, as the single particle tracking experiment is conducted at increasingly slower frame rates, the distances a GLUT1 can gradually move are more clearly resolved.

The microscopic diffusion coefficients (D_μ) of GLUT1 measured at five different frame rates are shown in Fig. 2. When recorded at 30 FPS, three well-separated populations of GLUT1 can be identified. A highly immobile (D_μ of 10^{-13} cm^2/s) population that might be hypothesized to be anchored to the junctional complex and comprises ~1/4 of the total GLUT1 proteins clearly constitutes the most immobilized subset. A somewhat more mobile, but still confined (D_μ of 10^{-11} cm^2/s) population that might be envisioned to be tethered to a more mobile site on the cortical spectrin cytoskeleton is then seen. This population comprises ~2/3 of the GLUT1 molecules. Finally, a small percentage of the population (~13%) that is rapidly moving (D_μ of 10^{-10} cm^2/s) and most likely freely diffusing in the membrane, constitutes the remainder of erythrocyte GLUT1.

3.3. Comparison of the mobilities of GLUT1 and band 3

Although the diffusion of band 3 has been extensively studied via single particle tracking at ≥120 FPS [10,11,12,13,22], fewer studies have investigated its diffusion at 30 FPS [23,24]. As seen in Fig. 3, the band 3 diffusion histogram resolves into a very broad single population of molecules at 30 FPS, probably arising from the overlap of the two or three major populations of band 3 (i.e. adducin-bound at the junctional complex, ankyrin-bound at the ankyrin complex, and unattached freely diffusing band 3) characterized in previous studies [11,12,13,22]. A comparison of band 3 to GLUT1 diffusion rates at 30 FPS shows striking differences. Most significantly, the least mobile subpopulation of GLUT1, comprising ~23% of GLUT1 molecules, diffuses with a D_μ centered at $8.5 \pm 0.8 \times 10^{-13}$ cm^2/s, a rate that is much slower than seen for any subpopulation of band 3.

While further studies will be required to confidently define the interactions responsible for each subpopulation of GLUT1, it is tempting to link the three diffusing subpopulations to the known binding partners of GLUT1 [5,6,7]. Because the least mobile subpopulation of GLUT1 diffuses with a D_μ that is slower than the junctional complex-tethered subpopulation of band 3, one might speculate that this most immobilized subpopulation of GLUT1 is anchored more tightly to the junctional complex than band 3. This could occur if GLUT1 were simultaneously tethered by both dematin and adducin; i.e. GLUT1's two known anchors to the junctional complex [5,25]. In contrast, the most mobile subpopulation of GLUT1 that comprises 13% of the total population exhibits a D_μ ($5.0 \pm 1.8 \times 10^{-10}$ cm^2/s) that is only 100-fold slower than the D_μ of most phospholipids ($1.6–9.4 \times 10^{-8}$ cm^2/s) [26], suggesting that it is either diffusing freely in the membrane or associated with lipid rafts, possibly through its known interaction with stomatin [7]; i.e. a common component of erythrocyte lipid rafts [27]. In support of this conjecture, Yan et al. have shown that a similar fraction (11%) of GLUT1 molecules directly colocalize with lipid rafts as seen by dSTORM imaging in HeLa cells [28]. Finally, since the majority of GLUT1 molecules display a D_μ ($1.8 \pm 0.1 \times 10^{-11}$ cm^2/s) similar to the major subpopulation of band 3 ($1.0 \pm 0.1 \times 10^{-11}$ cm^2/s), one might speculate that this remaining ~65% of GLUT1 molecules are tethered to the same junctional complexes as band 3, perhaps by only a single interaction with either dematin or adducin.

This conclusion, where one subpopulation of GLUT1 complexes appears to be similar to that of band 3, while other GLUT1 complexes appear to be different is, in fact, reinforced by the macroscopic diffusion rates and compartment size data. For example, as seen in Fig. 4 and Table 1, GLUT1 and band 3 macroscopic diffusion coefficients (D_M) are similar with a D_M of $6.3 \pm 0.2 \times 10^{-13}$ cm^2/s and $5.0 \pm 0.2 \times 10^{-13}$ cm^2/s, respectively suggesting similar complex mobilities. However, the compart size measurements (Fig. 4 and Table 1), where the diffusion of only the more immobilized subpopulations of GLUT1 and band 3 are monitored, show large differences between GLUT1 and band 3. That is, both GLUT1 and band 3 have immobilized subpopulations that are restricted to a ~35 nm compartment, however, only band 3 has a second subpopulation with a compartment size of 71 nm.

4. Conclusion

Current illustrations of the structure of the human erythrocyte membrane display two major complexes of membrane-spanning proteins [3,4], one comprised of band 3, band 4.1, glycophorins A and C, Duffy antigen, Kx, GLUT1, and stomatin, which are anchored directly or indirectly to the junctional complex, and a second containing band 3, glycophorin A, Rh proteins, CD47, LW, and glycophorin B tethered to the ankyrin complex. However, this standard depiction is almost certainly over-simplified. Thus, as demonstrated in this paper, GLUT1 exists in at least three different subpopulations, with other subpopulations obviously possible but not resolvable using our technique. While no information is available on the compositions of these subpopulations, they almost certainly correspond to interactions of GLUT1 with different membrane protein complexes, as the three populations are not likely different sized oligomers of GLUT1, since Saffman and Delbruck [29] have shown that changes in the cross-sectional area of a membrane-spanning protein will only change its diffusion coefficient by a factor proportional to the square root of the area increase. Thus, if a tetrameric GLUT1 were to associate into octamers, the diffusion coefficient would only decrease by 40%. Because the differences in D_μ are 3 orders of magnitude, these differences are almost certainly not solely due to different oligomeric forms of the transporter. By the same argument, small changes in the sizes of the GLUT1-containing membrane-spanning protein complexes cannot account for the changes in D_μ. Instead, the three subpopulations must derive from either major differences in the sizes of its membrane-spanning protein complexes or differences in their tethers to the spectrin-actin cytoskeleton (or both). Moreover, the fact that two of the motile subpopulations of GLUT1 do not coincide with the motile subpopulations of band 3 argues that at least two of the subpopulations of GLUT1 cannot be associated with band 3. Taken together, these data suggest that the standard diagrams of the human erythrocyte membrane remain oversimplified, even with the increasing complexity associated with each new iteration, suggesting that there is still a lot to learn about this simple model of human plasma membranes.

Acknowledgements

This work was supported by the National Institutes of Health [grant number GM024417].

References

[1] B. Alberts, A. Johnson, J. Lewis, et al., Molecular Biology of the Cell, 4th edition, Garland Science, New York, 2002 (Membrane Proteins).
[2] P. Gascard, N. Mohandas, New insights into functions of erythroid proteins in nonerythroid cells, Curr. Opin. Hematol. 7 (2) (2000) 123–129.
[3] S.E. Lux 4th, Anatomy of the red cell membrane skeleton: unanswered questions, Blood 127 (2) (2016) 187–199.
[4] T.J. Mankelow, T.J. Satchwell, N.M. Burton, Refined views of multi-protein complexes in the erythrocyte membrane, Blood Cells Mol. Dis. 49 (1) (2012) 1–10.
[5] A.A. Khan, T. Hanada, M. Mohseni, J.J. Jeong, L. Zeng, M. Gaetani, D. Li, B.C. Reed, D.W. Speicher, A.H. Chishti, Dematin and adducin provide a novel link between the spectrin cytoskeleton and human erythrocyte membrane by directly interacting with glucose transporter-1, J. Biol. Chem. 283 (21) (2008) 14600–14609.
[6] W. Jiang, Y. Ding, M. Jiang, X. Hu, Z. Zhang, Interaction of glucose transporter 1 with anion exchanger 1 in vitro, Biochem. Biophys. Res. Commun. 339 (4) (2006) 1255–1261.
[7] S. Rungaldier, W. Oberwagner, U. Salzer, E. Csaszar, R. Prohaska, Stomatin interacts with GLUT1/SLC2A1, band 3/SLC4A1, and aquaporin-1 in human erythrocyte membrane domains, Biochim. Biophys. Acta 1828 (3) (2013) 956–966.
[8] H. Shen, L.J. Tauzin, R. Baiyasi, W. Wang, N. Moringo, B. Shuang, C.F. Landes, Single particle tracking: from theory to biophysical applications, Chem. Rev. 117 (11) (2017) 7331–7376.
[9] A.E. Clark, G.D. Holman, Exofacial photolabelling of the human erythrocyte glucose

transporter with an azitrifluoroethylbenzoyl-substituted bismannose, Biochem. J. 269 (3) (1990) 615–622.
[10] G.C. Kodippili, J. Spector, C. Sullivan, F.A. Kuypers, R. Labotka, P.G. Gallagher, K. Ritchie, P.S. Low, Imaging of the diffusion of single band 3 molecules on normal and mutant erythrocytes, Blood 113 (24) (2009) 6237–6245.
[11] J. Spector, G.C. Kodippili, K. Ritchie, P.S. Low, Single molecule studies of the diffusion of band 3 in sickle cell erythrocytes, PLoS One 11 (9) (2016) e0162514.
[12] G.C. Kodippili, J. Spector, J. Hale, K. Giger, M.R. Hughes, K.M. McNagny, C. Birkenmeier, L. Peters, K. Ritchie, P.S. Low, Analysis of the mobilities of band 3 population associated with ankyrin protein and junctional complexes in intact murine erythrocytes, J. Biol. Chem. 287 (6) (2012) 4129–4138.
[13] G.C. Kodippili, J. Spector, G.E. Kang, H. Liu, A. Wickrema, K. Ritchie, P.S. Low, Analysis of the kinetics of band 3 diffusion in human erythroblasts during assembly of the erythrocyte membrane skeleton, Br. J. Haematol. 150 (5) (2010) 592–600.
[14] J. Gelles, B.J. Schnapp, M.P. Sheetz, Tracking kinesin-driven movements with nanometre-scale precision, Nature 331 (6155) (1988) 450–453.
[15] Y. Sako, A. Kusumi, Compartmentalized structure of the plasma membrane for receptor movements as revealed by a nanometer-level motion analysis, J. Cell Biol. 125 (6) (1994) 1251–1264.
[16] M.P. Sheetz, S. Turney, H. Qian, E.L. Elson, Nanometre-level analysis demonstrates that lipid flow does not drive membrane glycoprotein movements, Nature 340 (6231) (1989) 284–288.
[17] J.G. Powles, M.J.D. Mallett, G. Rickayzen, W.A.B. Evans, Exact analytic solution for diffusion impeded by an infinite array of partially permeable barriers, Proc. R. Soc. Lond. 436 (1992) 391–403.
[18] A. Kusumi, Y. Sako, M. Yamamoto, Confined lateral diffusion of membrane receptors as studied by single particle tracking (nanovid microscopy). Effects of calcium-induced differentiation in cultured epithelial cells, Biophys. J. 65 (1993) 2021–2040.
[19] M. Hashiramoto, T. Kadowaki, A.E. Clark, et al., Site-directed mutagenesis of GLUT1 in helix 7 residue 282 results in perturbation of exofacial ligand binding, J. Biol. Chem. 267 (25) (1992) 17502–17507.
[20] Y. Tamori, M. Hashiramoto, A.E. Clark, H. Mori, A. Muraoka, T. Kadowaki, G.D. Holman, M. Kasuga, Substitution at Pro385 of GLUT1 perturbs the glucose transport function by reducing conformational flexibility, J. Biol. Chem. 269 (4) (1994) 2982–2986.
[21] A. Muraoka, M. Hashiramoto, A.E. Clark, L.C. Edwards, H. Sakura, T. Kadowaki, G.D. Holman, M. Kasuga, Analysis of the structural features of the C-terminus of GLUT1 that are required for transport catalytic activity, Biochem. J. 311 (1995) 699–704.
[22] R. Mirchev, A. Lam, D.E. Golan, Membrane compartmentalization in Southeast Asian ovalocytosis red blood cells, Br. J. Haematol. 155 (1) (2011) 111–121.
[23] M. Tomishige, Y. Sako, A. Kusumi, Regulation mechanism of the lateral diffusion of band 3 in erythrocyte membranes by the membrane skeleton, J. Cell Biol. 142 (4) (1998) 989–1000.
[24] P. Karnchanaphanurach, R. Mirchev, I. Ghiran, J.M. Asara, B. Papahadjopoulos-Sternberg, A. Nicholson-Weller, D.E. Golan, C3b deposition on human erythrocytes induces the formation of a membrane skeleton-linked protein complex, J. Clin. Invest. 119 (4) (2009) 788–801.
[25] B. Machnicka, A. Czogalla, A. Hryniewicz-Jankowska, D.M. Bogusławska, R. Grochowalska, E. Heger, A.F. Sikorski, Spectrins: a structural platform for stabilization and activation of membrane channels, receptors and transporters, Biochim. Biophys. Acta 1838 (2) (2014) 620–634.
[26] T. Fujiwara, K. Ritchie, H. Murakoshi, K. Jacobson, A. Kusumi, Phospholipids undergo hop diffusion in compartmentalized cell membrane, J. Cell Biol. 157 (6) (2002) 1071–1081.
[27] U. Salzer, R. Prohaska, Stomatin, flotillin-1, and flotillin-2 are major integral proteins of erythrocyte lipid rafts, Blood 97 (4) (2001) 1141–1143.
[28] Q. Yan, Y. Lu, L. Zhou, J. Chen, H. Xu, M. Cai, Y. Shi, J. Jiang, W. Xiong, J. Gao, H. Wang, Mechanistic insights into GLUT1 activation and clustering revealed by super-resolution imaging, Proc. Natl. Acad. Sci. U. S. A. 115 (27) (2018) 7033–7038.
[29] P.G. Saffman, M. Delbruck, Brownian motion in biological membranes, Proc. Natl. Acad. Sci. U. S. A. 72 (8) (1975) 3111–3113.